

Isotope and Elemental Effects Indicate a Rate-Limiting Methyl Transfer as the Initial Step in the Reaction Catalyzed by *Escherichia coli* Cyclopropane Fatty Acid Synthase[†]

David F. Iwig, Anthony T. Grippe, Timothy A. McIntyre, and Squire J. Booker*

Department of Biochemistry and Molecular Biology, The Pennsylvania State University, University Park, Pennsylvania 16802

Received June 23, 2004; Revised Manuscript Received August 16, 2004

ABSTRACT: Cyclopropane fatty acid (CFA) synthases catalyze the formation of cyclopropane rings on unsaturated fatty acids (UFAs) that are natural components of membrane phospholipids. The methylene carbon of the cyclopropane ring derives from the activated methyl group of *S*-adenosyl-L-methionine (AdoMet), affording *S*-adenosyl-L-homocysteine (AdoHcys) and a proton as the remaining products. This reaction is unique among AdoMet-dependent enzymes, because the olefin of the UFA substrate is isolated and unactivated toward nucleophilic or electrophilic addition, raising the question as to the timing and mechanism of proton loss from the activated methyl group of AdoMet. Two distinct reaction schemes have been proposed for this transformation; however, neither was based on detailed in vitro mechanistic analysis of the enzyme. In the preceding paper [Iwig, D. F. and Booker, S. J. (2004) *Biochemistry* 43, <http://dx.doi.org/10.1021/bi048693+>], we described the synthesis of two analogues of AdoMet, *Se*-adenosyl-L-selenomethionine (SeAdoMet) and *Te*-adenosyl-L-telluromethionine (TeAdoMet), and their intrinsic reactivity toward polar chemistry in which AdoMet is known to be involved. We found that the electrophilicity of AdoMet and its onium congeners followed the series SeAdoMet > AdoMet > TeAdoMet, while the acidity of the carbons adjacent to the relevant heteroatom followed the series AdoMet > SeAdoMet > TeAdoMet. When each of these compounds was used as the methylene donor in the CFA synthase reaction, the kinetic parameters of the reaction, k_{cat} and $k_{\text{cat}}/K_{\text{M}}^{-1}$, followed the series SeAdoMet > AdoMet > TeAdoMet, suggesting that the reaction takes place via methyl transfer followed by proton loss, rather than by processes that are initiated by proton abstraction from AdoMet. Use of *S*-adenosyl-L-[methyl-*d*₃]methionine as the methylene donor resulted in an inverse isotope effect of 0.87 ± 0.083 , supporting this conclusion and also indicating that the methyl transfer takes place via a tight *s*_N2 transition state.

Cyclopropane fatty acids (CFAs)¹ exist naturally within the membrane structures of a wide variety of prokaryotes and several eukaryotes (1, 2). Ostensibly, their presence appears to relate little to the ecological niche of the respective

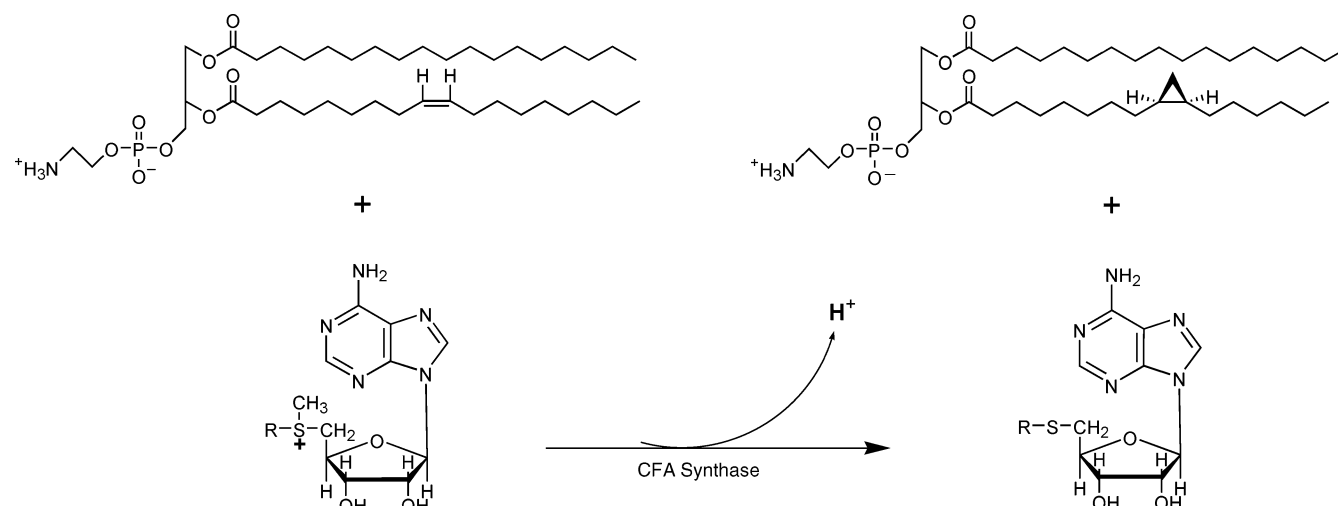
organism, since they are present in strict anaerobes, aerotolerant anaerobes, facultative anaerobes, microaerophiles, and obligate aerobes (1). Despite the predominance of CFA-producing organisms, the *raison d'être* of the cyclopropane modification is not completely understood in any system. In *Escherichia coli*, CFAs are found in fatty acids that comprise membrane phospholipids and are formed predominantly as the organism enters late-log and early-stationary phases of growth (3). This is attributed in part to the finding that transcription of the gene that encodes CFA synthase, the protein responsible for catalyzing CFA formation in *E. coli*, is partly under the control of the *rpoS* gene product, which is a σ factor that is essential for the expression of proteins that are present during stationary phase (4). Many of these proteins act in response to various types of environmental stress (4). Nevertheless, mutant strains of *E. coli* that are defective in CFA synthesis grow normally within the laboratory framework and appear to be as viable under a variety of stress conditions as the wild-type strain (5, 6). Recent work indicates that cyclopropane modifications in *E. coli* protect the bacterium from acid shock (7).

Cyclopropane rings are also found within the large ($\sim C_{70}$ – C_{90}), α -branched, β -hydroxylated fatty acids (mycolic acids)

[†] This work was supported by NSF Grant MCB-0133826.

* To whom correspondence should be addressed. Mailing address: 330 South Frear Laboratory, University Park, PA 16802. Phone: 814-865-8793. Fax: 814-863-7024. E-mail: sjb14@psu.edu.

¹ Abbreviations: AdoHcys, *S*-adenosyl-L-homocysteine; AdoMet, *S*-adenosyl-L-methionine; CFA, cyclopropane fatty acid; CMA, cyclopropane mycolic acid; COMT, catechol *O*-methyl transferase; DBA, 3,4-dihydroxybenzoic acid; DTT, dithiothreitol; EDTA, ethylenediaminetetraacetic acid; FAME, fatty acid methyl ester; FID, flame ionization detection; GC, gas chromatography; HEPES, *N*-(2-hydroxyethyl)piperazine-*N'*-2-ethanesulfonate; HPLC, high-performance liquid chromatography; IPTG, isopropyl- β -D-thiogalactopyranoside; ICP, inductively coupled plasma; IS, internal standard; LUV, large unilamellar vesicles; MTA, 5'-methylthioadenosine; MTase, methyltransferase; Ni-NTA, nickel nitrilotriacetic acid; PCR, polymerase chain reaction; PG, phosphatidylglycerol; PITC, phenylisothiocyanate; PL, phospholipid; PTH, phenylthiohydantoin; SeAdoHcys, *Se*-adenosyl-L-homoselenocysteine; SeAdoMet, *Se*-adenosyl-L-selenomethionine; Se-MTA, 5'-methylselenoadenosine; SOPG, 1-stearoyl-2-oleoyl-*sn*-glycero-3-[phospho-*rac*-(1-glycerol)]; TeAdoHcys, *Te*-adenosyl-L-homotellurocysteine; TeAdoMet, *Te*-adenosyl-L-telluromethionine; TeMTA, 5'-methyltelluroadenosine; TFA, trifluoroacetic acid; UFA, unsaturated fatty acid.

Scheme 1: The CFA Synthase Reaction^a

^a R = $-(\text{CH}_2)_2\text{CH}(\text{NH}_3^+)\text{COO}^-$.

of slow-growing pathogenic species of mycobacteria, such as *Mycobacterium tuberculosis* and *M. leprae*. Notably, few or no cyclopropane rings are found in the mycolic acids of saprophytic strains of mycobacteria such as *M. smegmatis* and *M. bovis* (8, 9). Moreover, strains of *M. tuberculosis* with null mutations in their *pcaA* gene, which encodes a cyclopropane mycolic acid (CMA) synthase, are unable to persist within infected mice and kill them, even though initial growth proceeds normally (10). In addition to affecting pathogenesis, cyclopropanation of mycolic acids decreases membrane permeability via a reduction in fluidity (11). This process has been associated with the ability of *M. tuberculosis* to resist treatments that utilize common antibiotics and chemotherapeutic agents, suggesting that CMA synthases may prove to be fruitful targets for the treatment of tuberculosis. Several CMA synthases are known, and CFA synthase from *E. coli* shares ~35% sequence identity and ~48% sequence similarity with these proteins, suggesting that the underlying mechanism of cyclopropanation is conserved in each case (12, 13).

CFAs are produced from the corresponding unsaturated fatty acid (UFA); the methylene carbon derives from the activated methyl substituent of *S*-adenosyl-L-methionine (AdoMet) (2). This is a *bi bi* reaction, in which two substrates, AdoMet and the UFA, interact to yield two products, *S*-adenosyl-L-homocysteine (AdoHcys) and the corresponding CFA, with concomitant release of a proton (Scheme 1). Two aspects of this reaction are especially noteworthy with respect to chemical and biochemical principles. First, CFA synthase is a soluble cytoplasmic enzyme, although it associates reversibly with the inner leaflet of cellular phospholipid bilayers (14). Interestingly, the unsaturated fatty acid substrate lies in the interior of the phospholipid bilayer and is presumably unexposed to the cytoplasm. The second substrate, AdoMet, is charged at all relevant pH values and highly soluble in aqueous solution and would not be expected to have ready access to the phospholipid bilayer interior. The manner in which the enzyme brings its two substrates of opposite solubilities in close proximity remains enigmatic. Second, the “business end” of the UFA substrate is an isolated and unactivated double bond that is always in the *cis* conformation; albeit,

trans cyclopropane synthase activity has been found in mycobacteria (2, 15). In vivo labeling studies in *Lactobacillus arabinosus*, which also contains a *cis* CFA synthase, revealed that both of the vinylic hydrogens of the substrate olefin are retained in the final product, suggesting that intermediates that involve loss of either of these hydrogens (e.g., cyclopropene, exomethylene, or methylalkene structures) were not operative (16). Transfer of the methylene group from AdoMet takes place with loss of only one of the original hydrogens; however, isotopic dilution has been observed in *L. plantarum* in vivo feeding studies (17).

Detailed mechanistic studies of the CFA synthase reaction have been limited because of the extreme lability of the enzyme. Since isolated olefins are generally both poorly nucleophilic and poorly electrophilic, any polar mechanism proposed would be at best only weakly satisfying. In solution chemistry, reactions of this nature usually proceed via carbene intermediates, which are rare in enzyme catalysis, unless the olefin is a Michael acceptor, which facilitates ylide-based mechanisms (18, 19). The central issue with respect to the mechanism of catalysis by CFA synthase concerns the timing and mechanism of proton loss from the activated methyl group of AdoMet. Two distinct working hypotheses have been advanced, but neither was based on detailed in vitro studies of purified protein. As early as 1963, the intermediacy of a sulfonium methylide was suggested, wherein the reaction is initiated by removal of one of the protons from the methyl substituent of AdoMet (20). The resulting carbanion would be stabilized by electrostatic interaction with the positively charged sulfur atom, delocalization of electron density into the empty d orbitals of the sulfur atom, or both (21). This proposal garnered momentum from a subsequent model study in which diphenylsulfonium methylide was shown to cyclopropanate various unactivated alkenes in the presence of a copper catalyst. The active cyclopropanating agent was postulated to be a copper-carbene complex generated after coordination of the ylide to the copper catalyst, with subsequent expulsion of diphenylsulfide (22).

In vivo studies on the biosynthesis of various sterols gradually led to a competing line of thought for the mechanism of cyclopropanation. Careful and detailed product

analyses from a host of feeding studies suggested that ergosterol, fucosterol, and various derivatives of 24-methylene sterols could all be biosynthesized from their respective olefinic precursor via a carbocation intermediate generated by electrophilic addition of the methyl substituent of AdoMet onto the π electrons of the olefin (19, 23, 24). In the vast majority of reactions, the carbocation produced would be tertiary, which is significantly more favorable than the secondary carbocation that would be generated if this mechanism were operative in CFA synthases. More recent investigations of the biosynthesis of mycolic acids in *M. tuberculosis* suggested that a similarly generated carbocation intermediate could account for the three major mycolic acid modifications of olefins that are formed by three structurally related enzymes: MMAS-4, which catalyzes formation of a secondary alcohol with an adjacent methyl branch, MMAS-3, which catalyzes the O-methylation of the secondary alcohol, and MMAS-2, which catalyzes cyclopropanation of the proximal *cis*-olefin of the mycolic acid substrate (25).

Herein, we describe experiments that distinguish between two mechanistic scenarios for the cyclopropanation of unactivated olefins by CFA synthase. We report the development of assays that allow detailed kinetic studies to be carried out on the enzyme, as well as those that allow direct observation of the cyclopropanated product. We establish that the enzyme neither binds divalent metal ions nor is inhibited by compounds that scavenge them. We use AdoMet and its onium congeners in combination with insight obtained from pH-dependent degradation studies of the compounds to show that the reaction takes place via a rate-limiting methyl transfer to the olefin followed by proton loss, rather than by processes that initiate with proton loss from AdoMet. Last, we show that α -secondary deuterium isotope effects are consistent with the model established by elemental effects, and further indicate a rate-limiting methyl transfer that takes place via a tight S_N2 transition state.

MATERIALS AND METHODS

Materials. All DNA modifying enzymes and reagents were purchased from New England Biolabs (Beverly, MA), as was Vent polymerase and its associated 10 \times reaction buffer. Oligonucleotide primers were obtained from Integrated DNA Technologies (Coralville, IA), while deoxynucleoside triphosphates were purchased from Amersham Pharmacia Biotech (Piscataway, NJ). Competent *E. coli* DH5 α cells were purchased from PGC Scientific (Gaithersburg, MD). *E. coli* (W3110) genomic DNA, methylthioadenosine (MTA), adenine, AdoHcys, catechol O-methyl transferase (COMT), 3,4-dihydroxybenzoic acid (DBA), potassium ferricyanide, 1,10-phenanthroline, and tryptophan were all purchased from Sigma (St. Louis, MO). The pET-28a(+) and pET-26b(+) plasmids and *E. coli* BL21(DE3)pLysS cells were purchased from Novagen (Madison, WI). Yeast extract and tryptone were purchased from Marcor Development Corporation (Hackensack, NJ). Kanamycin sulfate was purchased from Shelton Scientific (Shelton, CT). Isopropyl- β -D-thiogalactopyranoside (IPTG) was purchased from Biosynth International (Naperville, IL). Lysozyme, ethylenediaminetetraacetic acid (EDTA), and streptomycin sulfate were purchased from Fisher Biotech (Fair Lawn, NJ). Phenylisothiocyanate (PITC) and a high-purity amino acid calibration standard (Standard H) were purchased from Pierce (Rockford, IL). Nickel

nitrilotriacetic acid (Ni-NTA) resin was purchased from QIAGEN (Valencia, CA). 1-Stearoyl-2-oleoyl-*sn*-glycerol-3-[phospho-*rac*-(1-glycerol)] (SOPG) in chloroform was purchased from Avanti Polar Lipids, Inc. (Alabaster, AL). The metal powders, CoSO $_4$ ·6H $_2$ O, MnSO $_4$ ·H $_2$ O, NiSO $_4$ ·6H $_2$ O, and CuSO $_4$ ·5H $_2$ O, were all obtained from Aldrich (Milwaukee, WI), while a prepared iron standard (1000 μ g mL $^{-1}$ in 2% HNO $_3$) was obtained from SPEX CertiPrep (Metuchen, NJ). All solvents used for HPLC were of HPLC grade or better. All other chemicals and reagents were of the highest purity available and were purchased from Sigma or Aldrich unless noted otherwise.

AdoMet, *Se*-adenosyl-L-selenomethionine (SeAdoMet), and *Te*-adenosyl-L-telluromethionine (TeAdoMet) were synthesized as described in the preceding paper (26). *S*-Adenosyl-L-[methyl- d_3]methionine was synthesized in the same fashion using L-[methyl- d_3]methionine, which was obtained from Cambridge Isotope Laboratories, Inc (Andover, MA).

General Procedures. Routine UV-visible spectra were recorded on a Cary (Varian, Walnut Springs, CA) 300 Bio spectrophotometer using the associated Cary WinUV software package. High-performance liquid chromatography (HPLC) was carried out on an 1100 system from Agilent (Foster City, CA) with variable wavelength detection, while analysis by gas chromatography (GC) was carried out on an Agilent 6850 system with flame ionization detection (FID). Both instruments were equipped with autosamplers to facilitate the analysis of multiple samples. Sonic disruption of *E. coli* cells was carried out with a 550 sonic dismembrator from Fisher Scientific (Pittsburgh, PA) in combination with a horn containing a $1/2$ in. tip.

Conventional molecular biological manipulations were conducted using previously described standard procedures. DNA sequence determinations were performed by the Nucleic Acid Facility of the Penn State University Biotechnology Institute. Routine, small-scale plasmid preparations were carried out with the Promega (Madison, WI) Wizard kit, while large-scale plasmid preparations were carried out with Qiagen (Valencia, CA) Midi or Maxi kits. Removal and purification of DNA from agarose gels were performed with QIAquick gel extraction kits (Qiagen). The polymerase chain reaction (PCR) was conducted with a Robocycler temperature cycler from Stratagene (La Jolla, CA). Each amplification reaction contained the following in a volume of 100 μ L: 50 pmol of each primer, 20 nmol of each deoxynucleoside triphosphate, 2 μ g of *E. coli* (W3110) genomic DNA, 1 U of Vent polymerase, and 10 μ L of 10 \times Vent polymerase buffer. After a 5-min denaturation step at 95 $^{\circ}$ C, 35 cycles of the following program were initiated: 1 min at 95 $^{\circ}$ C, 1 min at 45 $^{\circ}$ C, and 2 min at 72 $^{\circ}$ C.

Construction of CFA Synthase Overexpression Strain. The gene for *E. coli* CFA synthase was amplified by PCR. The forward primer (5'-GCG-GCG-TCC-ATA-TGA-GTT-CAT-CGT-GTA-TAG-AAG-AAG-TC-3') was engineered to contain an *Nde*I restriction site (underlined) near its 5'-terminus, while the reverse primer (5'-GCG-GAA-TTC-TTA-GCG-AGC-CAC-TCG-AAG-GCC-G-3') was engineered to contain an *Eco*RI restriction site (underlined) near its 5'-terminus. After amplification and purification of the 1.1-kb fragment, it was digested with *Nde*I and *Eco*RI, and ligated into a pET-26a vector that had been similarly digested, resulting in plasmid pTAM100. An expression vector for His-tagged

(HT) CFA synthase was constructed by removing the *NdeI*–*EcoRI* fragment from pTAM100 and ligating it into a pET-28a vector that had been similarly digested, resulting in plasmid pATG125.

Growth and Overexpression of CFA Synthase. A single colony of *E. coli* BL21(DE3)pLysS containing plasmid pATG125 was used to inoculate 200 mL of 2×YT media (27) containing 50 $\mu\text{g mL}^{-1}$ of kanamycin sulfate and 0.1% dextrose. After the culture was allowed to grow at 37 °C for 8 h with shaking (225 rpm), four 25-mL aliquots were used to inoculate four 6-L Erlenmeyer flasks, each containing 2.5 L of the above media. The cultures were grown at 37 °C with agitation (225 rpm) until an OD_{600} of 0.6 was attained. IPTG was added to a final concentration of 40 μM , and the cultures were incubated further for 2 h in the same fashion. The cultures were chilled on ice for 30 min, and the cells were harvested at 4 °C by centrifugation at $10\,000 \times g$ for 10 min. The cell paste was immediately frozen in liquid nitrogen and stored at –80 °C. A typical yield was 2.5 g of wet cell paste per liter of culture.

Purification of CFA Synthase. All purification steps were carried out at 4 °C unless specifically noted, and all buffers were adjusted to a pH of 7.5 after incorporation of all components. In a typical purification, 25 g of cell paste was resuspended in 75 mL of lysis buffer (50 mM HEPES, 300 mM KCl, 10 mM imidazole, 10% glycerol) containing lysozyme at a final concentration of 1 mg mL^{-1} . After being stirred at room temperature for 20 min, the mixture was stirred in an ice–water bath until its temperature reached 8 °C or less (~15 min), and then subjected to four 30-s bursts of sonic disruption (35% output or 210 W) with intermittent pausing to maintain the temperature at ≤ 8 °C. The lysate was centrifuged for 1 h at $50\,000 \times g$ and 4 °C, and the resulting supernatant was loaded onto a Ni–NTA column (2.5 cm \times 5 cm). The column was washed with 10 column-volumes of wash buffer (50 mM HEPES, 300 mM KCl, 20 mM imidazole, 10% glycerol), before elution of CFA synthase with 30 mL of elution buffer (50 mM HEPES, 300 mM KCl, 250 mM imidazole, 10% glycerol). Fractions displaying significant absorbance at 280 nm were pooled and concentrated to ~300 μM by ultrafiltration using an Amicon stirred cell (Millipore; Billerica, MA) with a YM-10 membrane and exchanged into 100 mM HEPES (pH 7.5) by dialysis. The dialysate was combined with an equal volume of 50% glycerol, resulting in a final buffer composition of 50 mM HEPES (pH 7.5) and 25% glycerol. The protein, which was determined to be greater than 95% pure by SDS–PAGE with Coomassie staining, was frozen in liquid nitrogen and stored at –78 °C until ready for use. Its concentration was determined spectrophotometrically using an extinction coefficient that was determined in this work ($\epsilon_{280} = 70\,700 \text{ M}^{-1} \text{ cm}^{-1}$).

Molar Absorptivity Determination of CFA Synthase. A modified version of the amino acid analysis procedure of Heinrikson and Meredith was used to establish the molar absorptivity of CFA synthase at 280 nm (28). A UV–visible spectrum of a 1-mL sample of CFA synthase in 50 mM HEPES (pH 7.5) was recorded, and an aliquot (1.3 nmol) of the protein was hydrolyzed under vacuum in 6 N HCl for 24 h at 110 °C in a vacuum hydrolysis tube (Pierce, Rockford, IL). 3-Hydroxy-L-proline (40 μmol) was added as an internal standard before hydrolysis. Excess water and

acid were removed by centrifugal evaporation using a Thermo Savant (Milford, MA) SpeedVac concentrator, and the residue was dissolved in 50 μL of coupling buffer (10:5:2:3, acetonitrile/pyridine/triethylamine/water). The coupling buffer was evaporated in the same fashion, and the resulting residue was again dissolved in 50 μL of coupling buffer. A 5- μL aliquot of PITC was added, and the solution was allowed to stand at room temperature for 10 min. The coupling buffer and PITC were removed under vacuum, and the residue was dissolved in 10% methanol in water. Finally, the solvent was once again removed under vacuum, and the samples were dissolved in 10% methanol in 10 mM potassium phosphate buffer (pH 6.5). The hydrolysate was analyzed by HPLC using a Zorbax SB-CN column (5 μm , 4.6 mm \times 250 mm) with three solvents: 10 mM potassium phosphate buffer, pH 6.5 (solvent I), methanol (solvent II), and acetonitrile (solvent III). The sample was injected onto the column, which was equilibrated in 90% solvent I/10% solvent II, and the column was developed at a flow rate of 1 mL min^{-1} . After 15 min under the initial conditions, solvent III was increased from 0 to 32% over 32 min at the expense of solvent I, while maintaining solvent II at 10%. A calibration curve for several amino acids was generated by subjecting graded amounts of a standard solution of amino acids to derivitization and separation by the same procedure. The absolute concentration of CFA synthase was determined by dividing the concentrations of any of several amino acids in the protein hydrolysate by the number of times that the amino acid appeared in the CFA synthase sequence.

Construction of an AdoHcys Nucleosidase Overexpression Strain. The 699-bp *E. coli* AdoHcys nucleosidase gene (*pfs*) was amplified by PCR using two oligonucleotide primers that were complementary to the sequence at each end of the gene. The forward primer (5'-GCG-ACG-CAG-CAT-ATG-AAA-ATC-GGC-ATC-ATT-GGT-GCA-ATG-3') introduced a unique *NdeI* restriction site (underlined) at the 5'-terminus of the gene, while the reverse primer (5'-GCA-GGC-AGC-GAA-TTC-TTA-GCC-ATG-TGC-AAG-TTT-CTG-CAC-C-3') introduced a unique *EcoRI* restriction site (underlined) at the 3'-terminus of the gene. After amplification and purification of the 0.7-kb fragment, it was digested with *NdeI* and *EcoRI*, and ligated into a pET-28a vector that had been similarly digested, resulting in plasmid pATG134. The plasmid was subsequently transformed into *E. coli* strain BL21(DE3)pLysS for expression of the protein.

Overexpression of AdoHcys Nucleosidase. A single colony of *E. coli* BL21(DE3)pLysS containing plasmid pATG134 was used to inoculate 50 mL of 2×YT media containing 50 $\mu\text{g mL}^{-1}$ of kanamycin sulfate. After the culture was allowed to grow at 37 °C for 12 h with shaking (225 rpm), four 10-mL aliquots were used to inoculate four 6-L Erlenmeyer flasks, each containing 3 L of the above media. The cultures were grown at 37 °C with agitation (225 rpm) until an OD_{600} of 0.6 was attained. IPTG was added to a final concentration of 500 μM , and the cultures were incubated further for 3 h in the same fashion. The cultures were chilled on ice for 30 min, and the cells were harvested at 4 °C by centrifugation at $10\,000 \times g$ for 10 min. The cell paste was immediately frozen in liquid nitrogen and stored at –78 °C. A typical yield was 3 g of wet cell paste per liter of culture.

Purification of AdoHcys Nucleosidase. All purification steps were carried out at 4 °C unless specifically noted. In

a typical purification, 10 g of wet cell paste was resuspended in lysis buffer (50 mM HEPES, 300 mM KCl, 10 mM imidazole, 10% glycerol, pH 7.5) containing lysozyme at a final concentration of 1 mg mL⁻¹. After being stirred at room temperature for 20 min, the mixture was stirred in an ice-water bath until its temperature reached 8 °C or less (~15 min) and then subjected to four 30-s bursts of sonic disruption (35% output or 210 W) with intermittent pausing to maintain the temperature at ≤8 °C. The lysate was centrifuged for 1 h at 50 000 × g and 4 °C, and the resulting supernatant was loaded onto a Ni-NTA column (2.5 cm × 5 cm). The column was washed with 10 column-volumes of wash buffer (50 mM HEPES, 300 mM KCl, 20 mM imidazole, 10% glycerol, pH 7.5) before eluting AdoHcys nucleosidase with 30 mL of elution buffer (50 mM HEPES, 300 mM KCl, 250 mM imidazole, 10% glycerol, pH 7.5). Fractions displaying significant absorbance at 280 nm were pooled and concentrated by ultrafiltration using an Amicon stirred cell with a YM-10 membrane, and exchanged into 100 mM HEPES (pH 7.5) by dialysis. The dialysate was combined with an equal volume of 50% glycerol, rapidly frozen in aliquots with liquid N₂, and stored at -80 °C. The protein concentration was determined spectrophotometrically using an extinction coefficient ($\epsilon_{280} = 3140 \text{ M}^{-1} \text{ cm}^{-1}$) that was determined by the procedure of Gill and von Hippel (29).

Metal Analysis of CFA Synthase. Metal analysis was carried out by inductively coupled plasma (ICP) spectroscopy using a PS3000UV instrument from Leeman Labs (Hudson, NH). Standard solutions of each metal (Fe, Zn, Cu, Mn, Co, Ni, and P) ranging from 0.05 to 5 ppb were prepared and used to calibrate the ICP spectrometer prior to sample analysis. Concentrations of metal found in the protein sample were subsequently correlated to the protein concentration to determine the stoichiometry of each metal bound.

Preparation of Phospholipid Large Unilamellar Vesicles. SOPG (100–200 mg) in chloroform was placed in a 25-mL vial and subjected to rotary evaporation at 50 °C under reduced pressure (aspirator) to remove all traces of solvent. The remaining dry film of phospholipids was resuspended in 4–8 mL of 10 mM HEPES (pH 7.5) by intermittent vortexing for 2 h while spinning at 50 °C on a rotary evaporator without applied vacuum. The homogeneous mixture of phospholipids was subsequently subjected to three cycles of freezing at -80 °C and thawing at 37 °C. Large unilamellar vesicles (LUVs) were prepared by extrusion of the solution of phospholipids through polycarbonate filters (100 nm pore size) using a commercially available extruder from Avanti Polar Lipids, Inc (Alabaster, AL). The phospholipid concentration was determined by a previously described method (30), and the resulting vesicles were stored at room temperature and used within 10 h of preparation.

Activity Assays of CFA Synthase. The time-dependent formation of products in the CFA synthase reaction was monitored by HPLC or GC. A typical assay mixture contained the following in a final volume of 300 μ L: 50 mM HEPES (pH 7.5), 800 μ M AdoMet, 15 mM SOPG, 0.8 μ M CFA synthase, 0.5 μ M AdoHcys nucleosidase (specific activity 3.2 μ mol min⁻¹ mg⁻¹), and 1 mM tryptophan, which was used as an internal standard (IS). All components of the reaction mixture, excluding AdoMet, were incubated at 37 °C for 4 min prior to initiation of the reaction by addition

of AdoMet. Aliquots (40 μ L) were removed at various times, and the reaction was quenched by addition of H₂SO₄ to a final concentration of 50 mM. Samples were then stored at <4 °C until ready for analysis. Samples to be analyzed for adenine by HPLC were centrifuged (14 000 × g) to remove most of the phospholipids (PL), and a 10- μ L aliquot of the supernatant was injected onto an Agilent Zorbax SB-CN column (4.6 mm × 250 mm, 5 μ m) that was equilibrated in 95% solvent A (0.4% trifluoroacetic acid (TFA) in water, titrated to pH 1.8 with triethylamine) and 5% solvent B (methanol). Simultaneous linear gradients of 5–30% solvent B and 0–50% solvent C (acetonitrile) from 5 to 15 min gave good separation of AdoMet (3.15 min), adenine (4.5 min), AdoHcys (5.9 min), MTA (11.3 min), and the IS (12.9 min).

Assays to be analyzed by GC were carried out in a total volume of 2 mL. Aliquots (500 μ L) of the quenched reaction mixture were extracted three times with 400 μ L of *n*-hexane, and the hexane layers were pooled (1.2 mL) and incubated at room temperature with 100 μ L of 2 N NaOH in methanol for 10 min to form the fatty acid methyl esters (FAMES) of the corresponding phospholipids. The FAMES were concentrated under a stream of N₂, and 0.2- μ L aliquots were subjected to analysis by GC-FID using a DB-23 column (0.25 μ m, 60 m × 0.25 mm) from J & W Scientific (Folsom, CA). The injection port was maintained at 250 °C, while the detector was maintained at 280 °C. The initial column temperature was maintained at 50 °C for 1 min, raised to 175 °C over the following 5 min, and raised again to 230 °C over the following 13.75 min, resulting in a total run time of 19.75 min. Under these conditions, the saturated fatty acid (C18:0) eluted at 16.3 min, the unsaturated fatty acid (*cis*-C18:1) eluted at 16.7 min, and the cyclopropane fatty acid (*cis*-C18:1) eluted at 17.9 min. The concentration of the CFA product produced at each time point was calculated from eq 1,

$$[\text{CFA}] = [\text{S}]I_{\text{CFA}}/I_{\text{C18:0}} \quad (1)$$

wherein [S] is the concentration of the SOPG substrate and I_{CFA} and $I_{\text{C18:0}}$ are the integrated intensities of the peaks corresponding to CFA and C18:0, respectively. Initial rates as a function of substrate concentration were fitted to eq 2 by nonlinear regression,

$$v_0 = V_{\text{max}}[\text{S}]/(K_{\text{M}} + [\text{S}]) \quad (2)$$

wherein v_0 is the observed initial rate at a given substrate concentration [S], V_{max} is the maximal velocity of the reaction, and K_{M} is the apparent Michaelis constant for AdoMet.

Deuterium Isotope Effects. α -Deuterium isotope effects were measured by direct comparison of the kinetic constants obtained for [*methyl-d*₃]AdoMet and unlabeled AdoMet. Both substrates were synthesized and purified simultaneously, and their concentrations were determined spectrophotometrically ($\epsilon_{260} = 15\,400 \text{ M}^{-1} \text{ cm}^{-1}$). Reactions were carried out as described above for activity determinations, and initial rates at varying concentrations of AdoMet (5–500 μ M) were fitted to eq 2.

Activity Determination for Catechol O-Methyl Transferase. The general procedure for the activity determination of COMT was adapted from known methods (31). A typical

assay contained the following in a final volume of 220 μL : 50 mM HEPES, pH 7.5, 5 mM MgCl_2 , 5–200 μM AdoMet or SeAdoMet, 400 μM 3,4-dihydroxybenzoic acid (DBA), and 100 units of COMT. When reactions were conducted with TeAdoMet, its concentration was varied between 25 and 4000 μM , and 250 U of COMT were employed. Reactions were initiated by the addition of DBA after preequilibration of a mixture of all other components at 37 °C. At various times, 40- μL aliquots were removed and quenched with 10 μL of 125 mM H_2SO_4 . After precipitated protein was pelleted by centrifugation, 10- μL aliquots of the supernatant were analyzed by HPLC using the method described for separating the nucleoside products of the CFA reaction. Under these conditions, DBA eluted at 11.9 min, and 3-*O*-methyl DBA eluted at 13.2 min.

RESULTS

Expression, Purification, and Characterization of CFA Synthase. Previous studies of *E. coli* CFA synthase have vividly outlined the inherent difficulties associated with working with the enzyme (1, 14). In particular, CFAs or UFAs that serve as substrates appear to stabilize the enzyme, which can become problematic if they dissociate during conventional column chromatography. In the absence of phospholipids, the enzyme is completely inactivated upon incubation at 37 °C for 30 min and loses 50% of its activity at 4 °C during a period of ~16 h (14). Because of this lability, a strategy that would allow rapid purification of the enzyme was employed. The *cfa* gene was cloned into the *Nde*I site of a pET-28a vector, resulting in the production of protein containing a tandem six-histidine sequence (His-tag) separated from the natural N-terminus of the protein by a linker of 10 amino acids. Expression was carried out in *E. coli* BL21(DE3)pLysS as described previously—a procedure that minimizes inclusion body formation (32)—and the protein was purified to greater than 95% homogeneity by immobilized metal affinity chromatography (IMAC) using a Ni-NTA matrix. The protein was concentrated to ~200–250 μM , frozen in liquid N_2 , and stored at –78 °C in 25% glycerol. Under these conditions of storage, CFA synthase lost less than 10% percent of its initial activity after 6 months. Concentrating the protein to 300 μM or greater resulted in its precipitation from solution.

The UV-visible spectrum of purified CFA synthase is shown in Figure 1. Of note is the absence of distinct features at wavelengths greater than 320 nm, which is consistent with the absence of bound organic cofactors. A broad shoulder that extends throughout the spectral envelope is discernible and is attributed to light scattering by phospholipids that are tightly associated with the protein, which is described below.

Amino acid analysis using precolumn derivatization with PITC was carried out to establish a molar absorptivity for the protein at 280 nm. This was necessary because it could not be sufficiently concentrated to use the procedure of Gill and von Hippel, which requires substantial dilution in 6 M guanidine hydrochloride (29). The protein, corresponding to the UV-visible spectrum in Figure 1, was hydrolyzed in 6 N HCl under reduced pressure for 24 h at 110 °C, and the resulting amino acids in the hydrolysate were derivatized with PITC and separated by HPLC. Varying concentrations

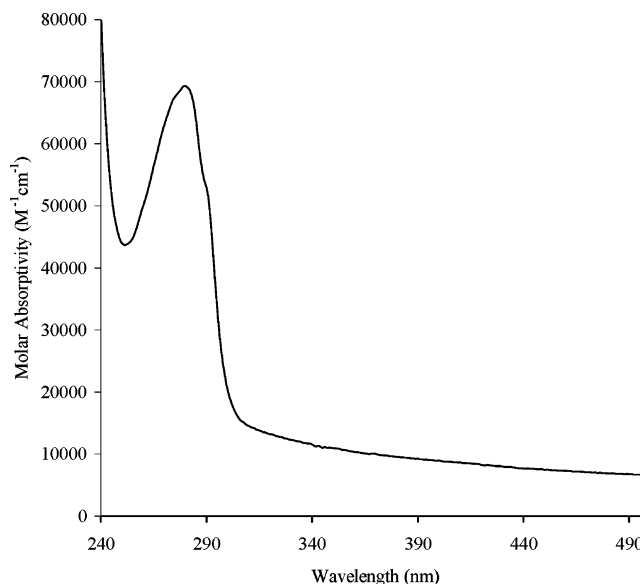


FIGURE 1: UV-visible spectrum of CFA synthase. The protein was diluted in 50 mM HEPES, pH 7.5, and 100 mM KCl. The broad tailing that is seen from 300 to 700 nm is attributed to light scattering by phospholipids that are bound tightly to the protein.

Table 1: Molar Absorptivities for CFA Synthase from Amino Acid Analysis^a

PTH-amino acid	calculated CFAS molar absorptivity ^b ($\text{M}^{-1} \text{cm}^{-1}$)
Ser	72 400 \pm 8 700
Gly	67 300 \pm 9 400
His	74 600 \pm 10 200
Met	73 600 \pm 9 100
Ile	73 900 \pm 7 800
Leu	66 500 \pm 9 100
Phe	69 100 \pm 8 500
Lys	68 000 \pm 5 100

^a Molar absorptivities were calculated as described in Materials and Methods. The mean CFA synthase molar absorptivity was determined to be $70\,700 \pm 3300 \text{ M}^{-1} \text{cm}^{-1}$. ^b Values are means of three separate determinations, and error is reported as \pm standard deviation.

of a commercially available amino acid mix were subjected to the same procedure to generate a calibration curve that was used to quantify the concentrations of select amino acids in the hydrolysate. Table 1 lists the amino acids that were chosen as standards, and the corresponding molar absorptivities that were calculated using the UV-visible spectrum shown in Figure 1. An average value of $70\,700 \pm 3300 \text{ M}^{-1} \text{cm}^{-1}$ was determined from these values.

Purified CFA synthase was analyzed for bound Ni, Fe, Zn, Mn, Co, Cu, and P by ICP spectroscopy (Table 2). Phosphorus was present in amounts that were stoichiometric with the protein (1.05 ± 0.21 equiv), while Fe, Zn, Mn, Co, Ni, and Cu were present at levels that were below, or only slightly above, the detection limit of the instrument. The finding of stoichiometric quantities of phosphorus suggests that the enzyme is isolated with phospholipids bound at the active site, which presumably accounts for its stability. It is possible also that the phosphorus is unrelated to phospholipids; however, GC-MS analysis indicated that fatty acids were indeed bound to the purified protein (data not shown).

Assay Development for CFA Synthase. HPLC- and GC-based procedures were developed to measure the activity of CFA synthase. In the reaction, two substrates are converted

Table 2: Results of Metal Analysis on CFA Synthase by ICP Spectroscopy^a

metal	metal/CFA synthase molar ratio
Fe	<0.01
Zn	<0.01
Mn	<0.01
Co	<0.01
Cu	<0.01
Ni	0.013
P	1.05 ± 0.21 ^b

^a Metal analysis was carried out as described in Materials and Methods. The concentration of CFA synthase in each sample was 2–100 μ M, and the detection limit of the instrument was 1 μ M. ^b The concentration of CFA synthase ranged from 33 to 88 μ M. The results are the average of four separate sample preparations. Error is reported as \pm standard deviation.

into three products. In the absence of uncoupling, turnover can be quantified by measuring the time-dependent loss of either of the two substrates, or the time-dependent accumulation of one of the three products. The HPLC-based procedure monitors the formation of adenine, which is derived from AdoHcys. AdoHcys is a product inhibitor of most methyl transferases (33) and inhibits CFA synthase with an apparent K_i of 220 μ M. Therefore, AdoHcys nucleosidase, which degrades AdoHcys to adenine and *S*-pentosylhomocysteine, was included in all assays to alleviate product inhibition. The GC-based procedure monitors the direct production of the CFA product; however, the HPLC-based procedure has a limit of detection of 1 μ M for adenine, making it more than 10-fold more sensitive than the GC-FID procedure. In addition, the GC-based method requires considerably more preparation before injection.

One caveat of the CFA synthase reaction involves the nature of the phospholipid substrate. In this study its concentration was maintained at very high levels in all assays (15 mM), which simplifies kinetic analysis of the reaction with the varied substrate (AdoMet). Nevertheless, heterogeneity in the nonvaried substrate, even when present at saturating concentrations, can complicate kinetic analysis of the reaction, especially if the nonvaried substrate binds before the varied substrate. The deviation from Michaelis–Menten behavior stems from the multiple enzyme forms to which the varied substrate can bind (34). Membrane phospholipids can vary in the nature of the headgroup, the nature of the fatty acid chains attached to their glycerol backbones, and the carbon on which any given fatty acid chain is bound (i.e. *sn*-1- or *sn*-2-position). The phospholipids present in membrane bilayers of *E. coli* are composed of 75% phosphatidylethanolamine (PE), 20% phosphatidylglycerol (PG), and 5% cardiolipin (CL) (35). CFA synthase is most active on phospholipids containing mixtures of headgroups; however, when only one headgroup is present, phosphatidylglycerol supports the highest level of activity (14). We elected, therefore, to use 1-stearoyl-2-oleoyl-*sn*-glycero-3-[phospho-*rac*-(1-glycerol)] (SOPG) as our model substrate, which contains a glycerol headgroup, a *cis*-9-octadecenoic fatty acid at the *sn*-2-position of the glycerophospholipid, and an octadecanoic fatty acid at the *sn*-1-position of the glycerophospholipid. In this fashion, only the fatty acid chain in the *sn*-2-position contains a substrate for the enzyme.

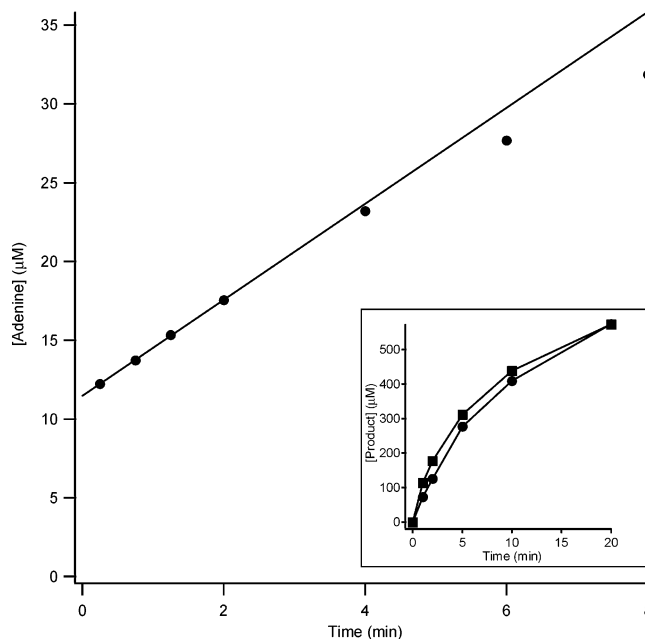


FIGURE 2: Typical CFA synthase activity assay trace showing formation of adenine over time. Reactions were carried out at 37 °C in 50 mM HEPES, pH 7.5, and contained 15 mM SOPG, 0.8 μ M CFAS, 0.5 μ M AdoHcys nucleosidase, 1 mM tryptophan (internal standard), and 500 μ M AdoMet. Aliquots were removed at various times and analyzed by HPLC as described in Materials and Methods. In the inset, the plot shows concomitant formation of adenine (■) and CFA methyl ester (●).

In Figure 2, a typical time-dependent trace of adenine formation is displayed. The rate of product formation is not linear for extended periods of time and begins to decline only after ~ 20 μ M CFAs are formed, despite the presence of millimolar concentrations of both substrates. This rapid decline in reaction rate before substantial amounts of substrate are consumed is not uncommon for enzymes that catalyze reactions at interfaces and usually indicates slow exchange of enzyme among phospholipid vesicles (36). In all activity determinations reported herein, only the initial linear portion of each trace (0–3 min) is used to obtain initial rates. Also apparent in Figure 2 is that the linear portion of the time course does not extrapolate back to 0 μ M adenine. AdoMet degrades nonenzymatically to adenine and MTA, which are common contaminants in most preparations of the compound (37–40). Any MTA present in the preparation or produced during the activity determination is rapidly converted to adenine by the MTA/AdoHcys nucleosidase that is included in each reaction. Each time point was corrected for adenine produced during the assay by processes that are unrelated to CFA synthase, according to eq 3, where $[A]_t$ is

$$[A]_c = [A]_t - [\text{AdoMet}]_0(1 - e^{-t(k_1+k_2)}) \quad (3)$$

the concentration of adenine at time t , $[A]_c$ is the concentration of adenine produced through the CFA synthase pathway, $[\text{AdoMet}]_0$ is the initial concentration of AdoMet, and k_1 ($5.1 \times 10^{-6} \text{ s}^{-1}$) and k_2 ($6.9 \times 10^{-6} \text{ s}^{-1}$) are the respective apparent first-order rate constants for the nonenzymatic degradation of AdoMet to adenine and MTA at pH 7.5 and 37 °C (26). When AdoMet was replaced with SeAdoMet, eq 3 was reduced to eq 4, since the nonenzymatic formation of adenine from SeAdoMet was negligible under the condi-

$$[A]_c = [A]_t - [\text{AdoMet}]_0(1 - e^{-k_2 t}) \quad (4)$$

tions of the assay; however, the apparent first-order rate constant for nonenzymatic formation of 5'-methylseleno-adenosine (SeMTA) was significantly greater ($k_2 = 8.5 \times 10^{-5} \text{ s}^{-1}$) (26).

TeAdoMet does not undergo significant nonenzymatic degradation under the conditions of the assay (26). However, the AdoHcys nucleosidase present in the assay unexpectedly catalyzed formation of adenine and *Te*-pentosyltelluromethionine from TeAdoMet but not the equivalent products from AdoMet or SeAdoMet (Figure 3). The turnover number (k_{cat}) for AdoHcys nucleosidase using TeAdoMet as a substrate was 0.112 min^{-1} , while the Michaelis constant (K_M) for TeAdoMet was $128 \mu\text{M}$. Therefore, when CFA synthase assays were conducted with TeAdoMet as the methylene donor, the initial rate (v_0) was determined from eq 5, wherein

$$v_0 = v_{\text{obs}} - \{ (k_{\text{cat}}[E][\text{TeAdoMet}]_0) / (K_M + [\text{TeAdoMet}]_0) \} \quad (5)$$

v_{obs} is the observed initial rate, $[E]$ is the concentration of AdoHcys nucleosidase, and $[\text{TeAdoMet}]_0$ is the starting concentration of TeAdoMet.

The inset to Figure 2 compares the relative concentrations of adenine and CFAs formed as a function of time. Typical GC and HPLC traces are provided in Supporting Information (Figures S3 and S1, respectively). It is important to note that the only peaks observed by GC are the methyl esters of C18:0, *cis*-C18:1, and cyclopropane C18:1, indicating that no intermediates or alternate products are formed to significant extents. At early time points, the concentrations of adenine and the CFA differ by as much as 30%; however, the amount of product observed by GC at early times is close to the limit of detection of the detector and in a range where the response is not linear. The hyperbolic nature of the curve derives from the relatively high concentrations of enzyme employed in the assay to detect the product by GC-FID. When AdoHcys nucleosidase was omitted from the reaction, the peak corresponding to adenine in the HPLC trace was significantly less intense, while a peak corresponding to AdoHcys became visible (Figure S2 in Supporting Information). The residual adenine is attributed to nonenzymatic degradation of AdoMet.

Effect of Additives on CFA Synthase. CFA synthase was assayed in the presence of agents that are capable of chelating metals or altering their oxidation states. The protein was incubated with each of the additives at 37°C for 5 min prior to initiating the reaction with AdoMet. As shown in Table 3, dithiothreitol (DTT), potassium ferricyanide, sodium dithionite, EDTA, and 1,10-phenanthroline had neither a stimulatory nor an inhibitory effect on the reaction within experimental error.

Effect of AdoMet, SeAdoMet, and TeAdoMet on the Kinetic Parameters of CFA Synthase and COMT. The effect of AdoMet and its onium congeners on the CFA synthase reaction in the presence of saturating concentrations of the UFA substrate is displayed in Figure 4. The corresponding Lineweaver–Burk plots are shown in the insets in each panel, and the extracted kinetic parameters from fits to eq 2 are listed in Table 4. When AdoMet was used as the cosubstrate

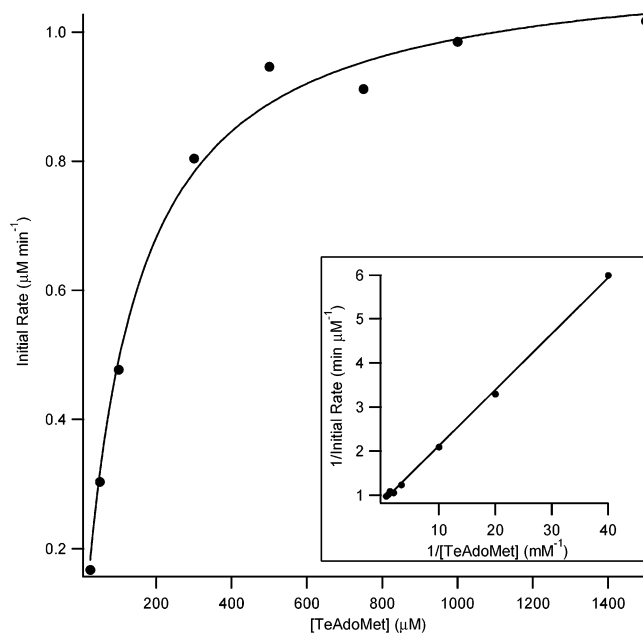


FIGURE 3: Concentration dependence of TeAdoMet on the initial rate of adenine formation by AdoHcys nucleosidase. Assays contained 50 mM HEPES, pH 7.5, 1 mM tryptophan as internal standard, $10 \mu\text{M}$ AdoHcys nucleosidase, and 0.1–1.4 mM TeAdoMet. Solid lines represent fits of initial rate data to eq 2. The inset shows a Lineweaver–Burk representation of the data.

Table 3: Dependence of CFA Synthase Activity on Metal Chelators, Oxidants, and Reductants^a

addition	concn (mM)	activity (%)
none		100
EDTA	1	113
1,10-phenanthroline	0.5	83
DTT	1	90
	10	91
sodium dithionite	2	112
	10	115
potassium ferricyanide	0.5	84
	5	121

^a Assays were carried out as described in Materials and Methods. Each reagent was incubated with CFA synthase at 37°C for 5 min before initiating the reaction by the addition of AdoMet. The percent activities are normalized against a typical assay containing no additions.

(Figure 4A), the associated turnover number and K_M value were $7.31 \pm 0.25 \text{ min}^{-1}$ and $89.4 \pm 12.8 \mu\text{M}$. Under the same conditions, SeAdoMet was a significantly better cosubstrate, displaying a turnover number of $13.0 \pm 0.4 \text{ min}^{-1}$ and a K_M value of $56.4 \pm 6.0 \mu\text{M}$ (Figure 4B). Last, TeAdoMet was a significantly worse cosubstrate, displaying a turnover number of $3.62 \pm 0.18 \text{ min}^{-1}$ and a K_M value of $740 \mu\text{M}$ (Figure 4C). When first-order (k_{cat}) or second-order rate constants ($k_{\text{cat}} K_M^{-1}$) are compared, the relative order of reactivity is SeAdoMet > AdoMet > TeAdoMet, SeAdoMet displaying a specificity constant ($k_{\text{cat}} K_M^{-1}$) that is 47 times that of TeAdoMet (Table 4).

The well-studied enzyme COMT displayed similar properties when assayed with AdoMet and its onium congeners (Table 5). Although the trend remains the same, the differences in the magnitudes of $V_{\text{max}} K_M^{-1}$ between AdoMet and SeAdoMet are less pronounced with COMT. By contrast, both of these compounds were significantly better cosubstrates than TeAdoMet, displaying second-order rates con-

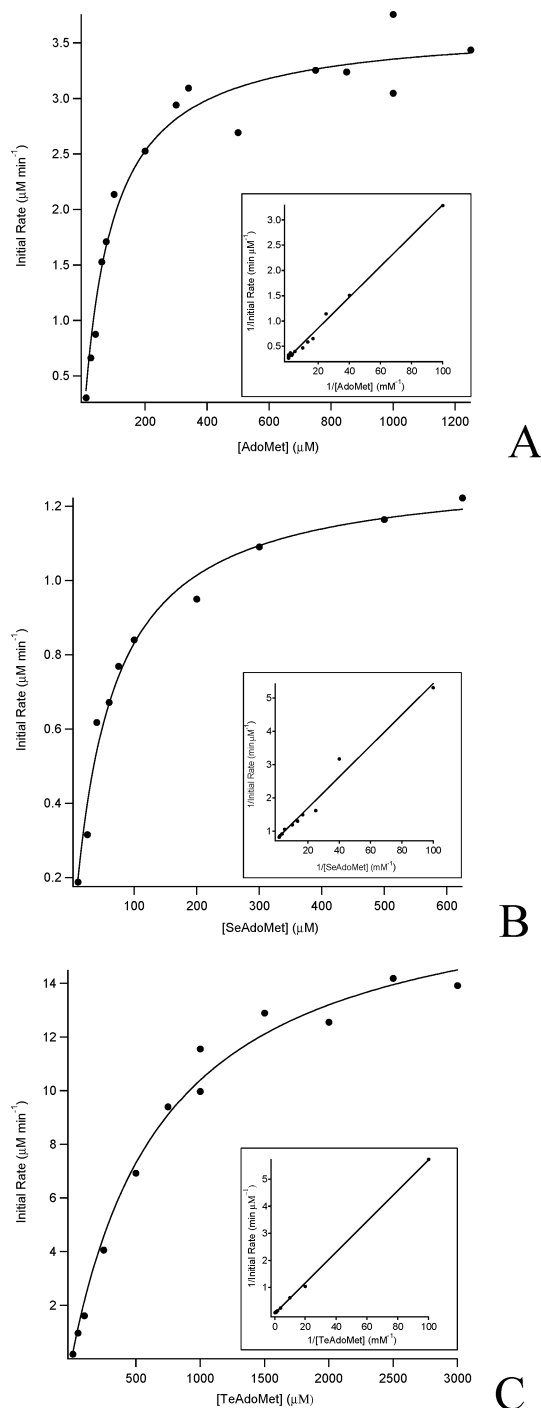


FIGURE 4: Concentration dependence of AdoMet (A), SeAdoMet (B), and TeAdoMet (C) on the initial rate of adenine formation by CFA synthase. Assays contained 50 mM HEPES, pH 7.5, 15 mM SOPG, 1 μ M AdoHcys nucleosidase, 10–1250 μ M AdoMet (A), 10–625 μ M SeAdoMet (B), or 10–3000 μ M TeAdoMet (C), and 0.5 (A), 0.1 (B), or 5 μ M (C) CFA synthase. Tryptophan (1 mM) was also included in each assay as an internal standard. Solid lines represent fits of initial rate data to eq 2. The insets show Lineweaver–Burk representations of the data.

stants that were greater than 100 times that of the tellurium-containing cosubstrate.

Deuterium Isotope Effects on the CFA Synthase Reaction. Reactions in which AdoMet was replaced with [methyl- d_3]-AdoMet were carried out to ascertain whether deuterium substitution at the activated methyl group of AdoMet would alter the kinetic properties of the reaction. Both compounds were synthesized and purified simultaneously and varied

Table 4: Kinetic Parameters of CFA Synthase with AdoMet, SeAdoMet, and TeAdoMet^a

substrate	K_M (μ M)	k_{cat} (min^{-1})	$k_{cat} K_M^{-1}$ ($\mu\text{M}^{-1} \text{min}^{-1}$)
AdoMet	89.4 ± 12.8	7.31 ± 0.25	0.0818 ± 0.012
SeAdoMet	56.4 ± 6.0	13.0 ± 0.4	0.230 ± 0.025
TeAdoMet	740 ± 102	3.62 ± 0.18	0.00489 ± 0.00072

^a Assays were carried out as described in Materials and Methods. The data were fitted to eq 2 to extract the above kinetic parameters. Error is reported as \pm standard deviation.

Table 5: Kinetic Parameters of COMT with AdoMet, SeAdoMet, and TeAdoMet^a

substrate	K_M (μ M)	V_{max} (nM min^{-1}) ^b	$V_{max} K_M^{-1}$ (min^{-1}) ^b
AdoMet	4.92 ± 0.44	7.92 ± 0.11	0.00161 ± 0.00015
SeAdoMet	4.61 ± 0.65	8.89 ± 0.17	0.00193 ± 0.00027
TeAdoMet	87.5 ± 11.0	1.25 ± 0.03	0.0000143 ± 0.0000018

^a Assays were carried out as described in Materials and Methods. Data were fitted to eq 2 to extract the above kinetic constants. Error is reported as \pm standard deviation. ^b Values are reported in V_{max} and $V_{max} K_M^{-1}$ because the enzyme was obtained as an impure preparation. All values were normalized to the number of units of COMT added.

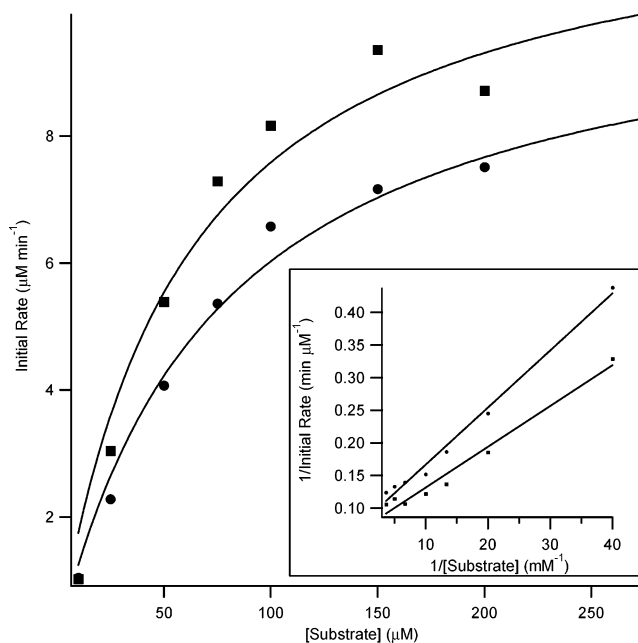
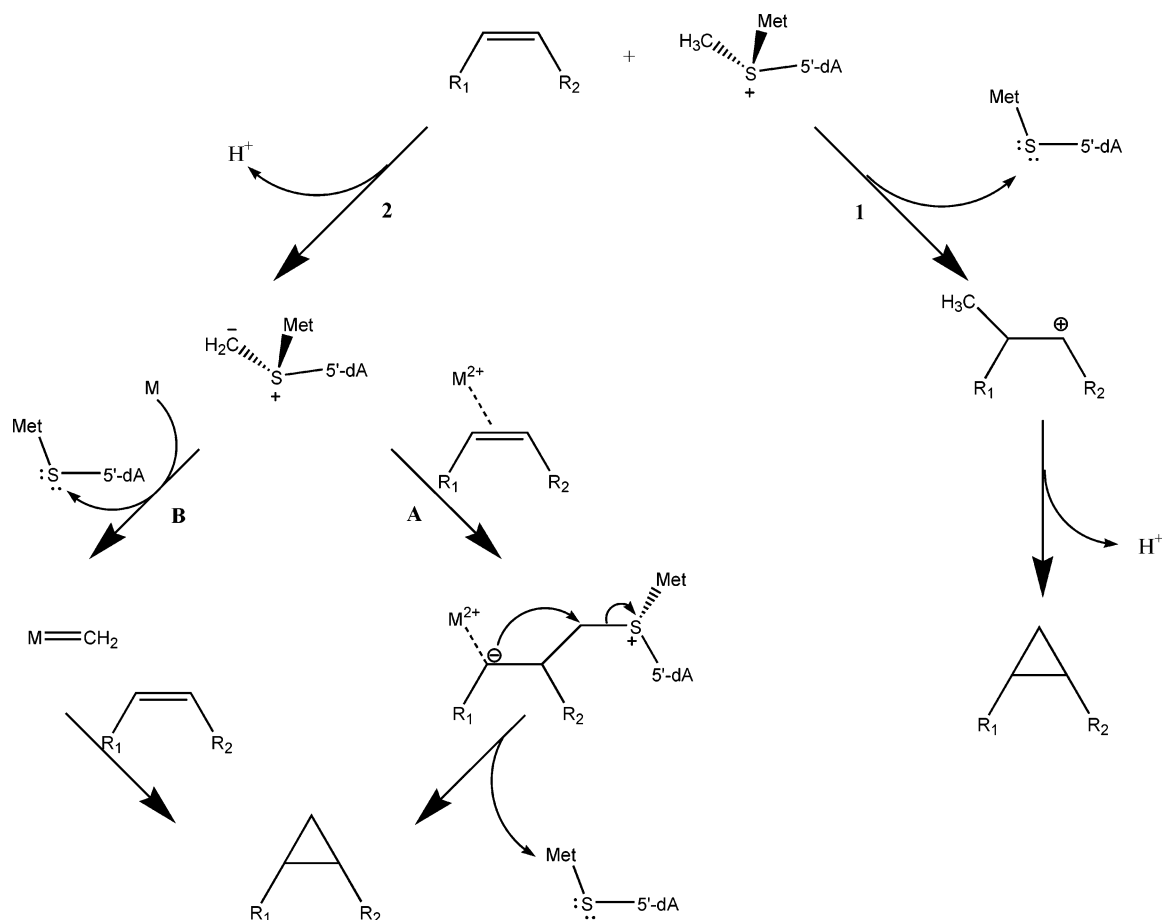


FIGURE 5: Concentration dependence of AdoMet (●) and [methyl- d_3]-AdoMet (■) on the initial rate of adenine formation by CFA synthase. Assays contained 50 mM HEPES, pH 7.5, 15 mM SOPG, 0.8 mM CFAS, 1.0 mM AdoHcys nucleosidase, and 10–250 mM AdoMet or [methyl- d_3]-AdoMet. Tryptophan (1 mM) was also included as an internal standard. Solid lines represent fits of initial rate data to eq 2. The insets show Lineweaver–Burk representations of the data.

from 5 to 500 μ M at saturating concentrations of the UFA substrate. In Figure 5, initial rates, plotted as a function of AdoMet or [methyl- d_3]-AdoMet concentration are displayed with the associated Lineweaver–Burk plots presented in the inset. Fits of the initial-rate data to eq 2 yielded k_{cat} and K_M values of 11.8 ± 0.6 and 53 ± 9.3 , and 13.6 ± 0.5 and 54.4 ± 8.4 for AdoMet and [methyl- d_3]-AdoMet, resulting in an isotope effect of 0.87 ± 0.083 on k_{cat} and 0.88 ± 0.07 on $k_{cat} K_M^{-1}$ (Table 6). Repetition of the experiment gave an isotope effect of 0.86 ± 0.09 on k_{cat} .

Scheme 2: Working Models for CFA Synthase Reaction

Table 6: Kinetic Parameters of α -Deuterium Isotope Effect on CFA Synthase Activity^a

substrate	K_M (μM)	k_{cat} (min^{-1})	$k_{\text{cat}} K_M^{-1}$ ($\mu\text{M}^{-1}\text{min}^{-1}$)
AdoMet	53.1 ± 9.3	11.8 ± 0.6	0.222 ± 0.040
[methyl- d_3]AdoMet	54.4 ± 8.4	13.6 ± 0.5	0.250 ± 0.040

^a Isotope effects were measured from direct comparison of the kinetic constants obtained with AdoMet and [methyl- d_3]AdoMet as described in Materials and Methods. The calculated isotope effect on k_{cat} is 0.87 ± 0.083 .

DISCUSSION

Characterization of CFA Synthase. CFA synthase is unique among enzymes that employ AdoMet as a cosubstrate; it catalyzes the net transfer of a methylene group, rather than a methyl group, to an isolated and unactivated olefin. The manifest goal of the research described herein was to address the timing of proton loss from the activated methyl group of AdoMet to distinguish among several reasonable models for catalysis that have been advanced. In Scheme 2, the two mechanistic possibilities that served as a framework for this study are displayed. In pathway 1, direct methyl transfer to the olefin substrate would afford a methyl-cation intermediate, which upon loss of a proton could cyclize, forming a cyclopropane ring. Alternatively, loss of a proton from the activated methyl group of AdoMet would give rise to a sulfonium methylide, which could react by at least two mechanisms (pathway 2). Direct attack of the carbanion onto the olefin would transfer the negative charge to the fatty acid, affording a cyclopropane ring upon reattack of the carbanion

onto the bridging methylene (formerly methyl) carbon of AdoMet with concomitant expulsion of AdoHcys (pathway 2A). Or, as described in Pathway 2B, the ylide could serve as a precursor to a carbene intermediate as proposed previously for this reaction (22).

Pathway 1 has little or no precedent in solution chemistry. Conversely, there is significant chemical precedent for the use of sulfonium ylides to form cyclopropane rings; however, such reactions typically require suitably polarized electrophiles such as Michael acceptors (18). Carbenes and carbenoids are well-appreciated intermediates in cyclopropanation reactions (18). We postulated that if CFA synthase catalyzed its reaction via formation of an ylide, the protein might also harbor a metal ion, either to polarize the double bond for nucleophilic attack via asymmetric coordination or to participate in the formation of a metal carbene species. Analyses for Cu, Zn, Co, Fe, Ni, and Mn, common transition metals found in biology, indicated that they were not associated with the protein in amounts that were significantly above the detection limit of the ICP spectrometer. However, phosphorus was detected in quantities that were stoichiometric with enzyme, which was attributed to the presence of tightly bound phospholipids.

One point of concern was that the activity observed was perhaps attributable to a minute fraction of enzyme containing bound metal, which goes undetected in metal analyses. Attempts to establish the concentration of active protein by ascertaining whether a burst of product (AdoHcys) preceded the normal steady-state rate of product production were unsuccessful. Burst kinetics was not observed. Several other

lines of evidence, however, suggest that activity is not attributable to minute amounts of metal-containing enzyme. First, treatment of CFA synthase with metal chelators such as EDTA and *o*-phenanthroline had little or no effect on turnover. Second, agents such as potassium ferricyanide and sodium dithionite, which might oxidize or reduce a bound metal ion, rendering it incapable of carrying out its normal function, had little or no effect on turnover. Last, the turnover number reported herein for CFA synthase (7.31 min^{-1} with AdoMet as the cosubstrate) agrees well with those of other AdoMet-dependent methyltransferases (MTases), which typically catalyze relatively slow reactions. For example, the turnover number for COMT is $\sim 60 \text{ min}^{-1}$ for methylation of the hydroxyl group at C-3 and $\sim 6\text{--}12 \text{ min}^{-1}$ for methylation of the hydroxyl group at C-4, whereas the turnover number for glycine N-MTase is $\sim 6 \text{ min}^{-1}$ (41) and that for guanidinoacetate MTase is 4.86 min^{-1} (42). DNA MTases tend to have even lower turnover numbers under steady-state conditions; however, methyl transfer often is not the rate-limiting step. Pre-steady-state studies have allowed rate constants for only the methyl transfer step to be extracted in a number of systems. For example, *HhaI* DNA-(cytosine-C⁵)-MTase has a $k_{\text{methylation}}$ of $\sim 15.6 \text{ min}^{-1}$ (43), whereas *BamHI* DNA-(cytosine-N⁴)-MTase from *Bacillus amyloliquefaciens* and bacteriophage T4Dam DNA-(adenine-N⁶)-MTase have $k_{\text{methylation}}$ s of 5.1 and 33.6 min^{-1} , respectively (44). It must be mentioned that the *EcoRI* DNA-(adenine-N⁶)-MTase has a $k_{\text{methylation}}$ of 2460 min^{-1} (45); however, this rate constant is generally not representative of those of most methyltransferases. Of all methyltransferases, the nucleophile in the CFA reaction is perhaps the least reactive. In cytosine-C⁵-MTases, another example of methyl transfer to carbon atoms, a conserved cysteine residue drives the reaction via nucleophilic addition to the double bond that is to accept the methyl group (46, 47). These significant points suggest that a substantial fraction, if not all, of our CFA synthase preparation is indeed in an active form and therefore lead us to conclude that CFA synthase does not employ a metal in catalysis, which casts doubt on the plausibility of ylide formation as a key step in its mechanism.

Elemental Effects on the CFA Synthase Reaction. Our model studies in the preceding paper (26) should allow us to predict relative reactivities of AdoMet, SeAdoMet, and TeAdoMet in AdoMet-requiring reactions if the relevant chemistry is involved in the rate-determining step of the reaction. These “elemental effects” have been used extensively in the analysis of phosphoryl transfer reactions to dissect their kinetic mechanisms (48, 49). In such instances, substitution of a sulfur atom for one of the oxygen atoms on the phosphate to be transferred typically results in a retardation of the step, stemming from a combination of steric and electronic effects. However, inverse “thio effects” also have been observed (50). Thio effects can allow determination of the rate-limiting step in a reaction; however, a number of caveats associated with using them as such have been registered (49).

Onium chalcogen effects were employed herein to address the timing of proton loss from the activated methyl group of AdoMet. As described above, and detailed in Scheme 2, the question that was posed was whether the proton is removed from the activated methyl group of AdoMet while it is still bonded to the sulfur atom. In the preceding paper

(26), the intrinsic reactivities of AdoMet and its onium congeners in aqueous solution as a function of pH were assessed. Their relative electrophilicities were determined by monitoring the formation of MTA, 5'-methylselenoadenosine (SeMTA), or 5'-methyltelluroadenosine (TeMTA), which derive from intramolecular attack of the carboxylate of AdoMet, SeAdoMet, or TeAdoMet onto the respective γ carbon. Their relative acidities were assessed by monitoring formation of adenine, which results from deprotonation at C-5', with a subsequent α/β elimination to generate an aldehyde at C-1' concomitant with cleavage of the glycosidic bond (51). Analysis of the pH-dependent data allowed extraction of apparent pK_a values of ~ 11.5 and ~ 14.1 for deprotonation at C-5' of AdoMet and SeAdoMet, a difference of $\sim 2.6 pK_a$ units. Marcus theory (52) allows prediction of rate constants for proton abstraction as a function of the separation in the pK_a values (ΔpK_a) between the general-base catalyst in the reaction and the proton to be abstracted (53, 54). Equation 6 describes this relationship, wherein k is

$$k = (k_B T/h) \exp\{ -[(\Delta G^\ddagger/(RT)) + 2.303 \Delta pK_a] \} \quad (6)$$

the rate constant for proton abstraction, k_B is Boltzmann's constant, T is the temperature in Kelvin, h is Planck's constant, R is the universal gas constant, and ΔG^\ddagger is the intrinsic barrier to isoergonic proton transfer. Assuming that ΔG^\ddagger is relatively equal for proton abstraction from AdoMet as compared to SeAdoMet, it can be shown that a difference of $2.6 pK_a$ units would correspond to a ~ 400 -fold decrease in k when AdoMet is replaced with SeAdoMet. The assumption that ΔG^\ddagger is relatively equal for AdoMet versus SeAdoMet derives from their steric and electronic similarities. As an internal check of the validity of this assumption, the ratios of the rate constants for adenine formation from AdoMet and SeAdoMet at pH 10.5 and pH 12 were found to be 435 and 471, in fair agreement with the calculated ratio (26). The finding that the CFA synthase reaction proceeds almost *twice as fast* with SeAdoMet than with AdoMet, therefore, argues against proton abstraction from the activated methyl group while it is attached to the chalcogen.²

Although the apparent pK_a values established in our solution studies are not intrinsic (microscopic) pK_a values, there is evidence that the differences in the intrinsic pK_a values of protons adjacent to sulfonium versus selenonium groups vary to similar extents. A recent analysis of the effects of adjacent onium cations on the equilibrium acidities of select compounds in dimethyl sulfoxide solution revealed the pK_a values of $\text{C}_6\text{H}_5\text{CH}_2\text{S}^+\text{Bu}_2\text{Br}^-$, $\text{C}_6\text{H}_5\text{CH}_2\text{Se}^+\text{Bu}_2\text{Br}^-$, and $\text{C}_6\text{H}_5\text{CH}_2\text{Te}^+\text{Bu}_2\text{Br}^-$ to be 18.8, 23.5, and 23.8 (21). In addition, the pK_a of the trimethylsulfonium ion in water has been estimated to be 18.9 (55).

Substitution of SeAdoMet for AdoMet in the CFA synthase reaction resulted in a 2-fold enhancement in k_{cat} and a ~ 3 -fold enhancement in $k_{\text{cat}} K_M^{-1}$, while substitution with TeAdoMet resulted in a 2-fold reduction in k_{cat} and a ~ 17 -fold reduction in $k_{\text{cat}} K_M^{-1}$. As detailed above, this trend is inconsistent with a rate-limiting proton abstraction to form

² Recent work from the laboratory of Dr. Hung-wen Liu using fatty-acid analogues of phospholipids is also consistent with a carbocation mechanism for CFA synthase [Molitor, E. J., Paschal, B. M. and Liu, H.-W. (2003) *ChemBioChem* 4, 1352–1356].

a sulfonium methylide but is consistent with our findings on the relative electrophilicity of the three compounds in water. Although a detailed kinetic analysis of this enzyme has yet to be carried out, all AdoMet-dependent MTases follow sequential mechanisms, and it is highly likely that CFA synthase is similar. Under initial rate conditions and in the presence of saturating concentrations of substrates, k_{cat} can be expressed in terms of all of the first-order rate constants in the reaction, including those governing the release of products. Therefore, upon substitution of SeAdoMet for AdoMet, the increase in k_{cat} could reflect faster release of SeAdoHcys from the product complex or faster conversion of the UFA–SeAdoMet complex to the CFA–SeAdoHcys complex. Our failure to observe a burst under pre-steady-state conditions in our kinetic studies suggests that product release is not rate-limiting and that changes observed are related to the chemical step. The finding that the reaction proceeds at a faster rate with SeAdoMet, but at a slower rate with TeAdoMet would argue against an increase in the rate constant associated with some other type of nonchemical step, such as a conformational change.

Elemental Effects on COMT. To add credence to our findings, the response of COMT to onium chalcogens of AdoMet was assessed. COMT is perhaps the best-characterized AdoMet-dependent MTase. The kinetic mechanism is ordered-sequential; AdoMet binds first, followed sequentially by Mg^{2+} and catechol, while the release of products follows the reverse order (31). Importantly, methyl transfer is rate-limiting (56). When SeAdoMet was substituted for AdoMet in this system, a ~ 1.1 -fold enhancement in k_{cat} and a ~ 1.2 -fold enhancement in $k_{\text{cat}} K_{\text{M}}^{-1}$ was observed, while substitution with TeAdoMet resulted in a 6.3-fold reduction in k_{cat} and a ~ 112 -fold reduction in $k_{\text{cat}} K_{\text{M}}^{-1}$. Although the effects are not as dramatic as those observed with CFA synthase on SeAdoMet substitution, the most important aspect of this study is that there was no significant decrease in k_{cat} , which would be expected if proton abstraction from SeAdoMet were a key step in catalysis.

Presently, very little can be extracted from the absolute magnitudes of onium chalcogen effects in enzyme systems because of a lack of relevant model studies to ascertain to what extent they can vary. In our model studies, SeAdoMet was 10-fold more reactive as an electrophile than AdoMet; however, in the two different enzyme systems addressed in this study, the effect on k_{cat} varied between 1.1 and 1.8. The difference may be partly attributable to solvation effects. In water, the medium in which the model studies were carried out, the ground state for AdoMet may be further lowered as compared to SeAdoMet because of better solvation of the sulfonium ion versus the selenonium ion.

Deuterium Isotope Effects on CFA Synthase. To substantiate the conclusions drawn from elemental effects, isotope effect studies on the CFA synthase reaction using [*methyl-d*₃]AdoMet were carried out. We postulated that if ylide formation were operative and rate-limiting, a primary isotope effect on C–H bond cleavage should be observed. By contrast, if methyl transfer were operative and fully rate-limiting, a small α -secondary isotope effect on the reaction would be expected, the value and nature of which would depend on the nature of the transition state for transfer. An inverse isotope effect of ~ 0.87 on both V_{max} and $V_{\text{max}} K_{\text{M}}^{-1}$ was observed. A similar isotope effect (0.83 ± 0.05) was

observed on COMT-catalyzed methyl transfer by Hegazi, Borchardt, and Schowen using [*methyl-d*₃]AdoMet. This isotope effect, in combination with the ^{13}C isotope effect on V_{max} of 1.09 ± 0.05 allowed them to conclude that methyl transfer was rate-limiting and that it proceeded via a “tight” transition state, wherein there is substantial bonding of the nucleophile and the leaving group to the central atom (56). Ideally, we would have liked to determine the ^{13}C isotope effect on k_{cat} to strengthen our argument; however, in contrast to the studies on COMT, the precision of our assay did not allow a reliable direct comparison of rates that might differ by less than 5%.

Conversion of the Methyl-Cation Intermediate to the Cyclopropane Product. Buist and MacLean arrived at a similar conclusion in their *in vivo* feeding studies on the transfer of deuterium to CFAs from isotopically labeled L-methionines (17). Using [*methyl-d*₃]-, [*methyl-d*₂]-, and [*methyl-d*₁]-methionine, they were able to calculate a minimum intramolecular isotope effect of 3.6 ± 0.2 on the transfer of deuterium to CFAs. The absence of an intermolecular isotope effect (1.01 ± 0.04) when *L. plantarum* was fed a 1:1 mixture of L-methionine and L-[*methyl-d*₃]-methionine led them to conclude that C–H bond cleavage is not rate-determining in the cyclopropanation reaction. Important among their observations was that about one-third of all CFAs generated in their *in vivo* feeding studies had exchanged protons in their cyclopropane rings, which was not a result of nonenzymatic exchange from AdoMet. They concluded that these results were most consistent with a rate-limiting methyl transfer to the olefin, resulting in a carbonium ion intermediate, followed by a relatively fast and reversible deprotonation of the methyl-cation intermediate to afford the cyclopropane ring.

We invoke the intermediacy of a protonated cyclopropane ring as our working hypothesis for the deprotonation of the methyl-cation species (Scheme 2). These are well-known intermediates in the rearrangement of various carbonium ions, the simplest of which is the 2-propyl cation (57). In addition, they have been invoked in the biosynthesis of various marine sterols (58–60), as well as the catalytic-antibody-induced cyclization of a high-energy cationic intermediate (61, 62). Equilibrium constants have been measured for proton transfers between protonated methanol ($\text{p}K_{\text{a}}$ ca. -2) and cyclopropane, as well as protonated formic acid ($\text{p}K_{\text{a}}$ ca. -4) and cyclopropane in the gas phase (63), and are 0.484 and 3.65 (64), respectively, suggesting that the $\text{p}K_{\text{a}}$ of a protonated cyclopropane ring is ca. -2 to -4 . The equilibrium constant between protonated methanol and methylcyclopropane is 2.85, which would result in a slightly higher $\text{p}K_{\text{a}}$ for protonated methylcyclopropane than for protonated cyclopropane.

Recently, the crystal structures of three CMA synthases from *M. tuberculosis* have emerged and have shed light on how an enzyme active site might be engineered to effect a reaction that does not take place in solution (65). In particular, a structure of CMA1 bound with cetyltrimethylammonium bromide and AdoHcys is most informative, since the former mimics the fatty acid substrate while the latter mimics AdoMet. Although turnover in an assay system with purified enzyme has not been reported for any CMA synthase, several aspects of the structure deserve particular mention. Since both substrates are bound to the enzyme

simultaneously, a sequential rather than ping-pong mode of catalysis would be operative. The active site is composed primarily of aromatic amino acids, the majority of which are tyrosines. The face of the aromatic ring of Tyr-33 is 4.9 Å away from the positive charge on the substrate analogue and is postulated to contribute to transition state stabilization in the normal reaction via a π -cation interaction (65, 66). Unexpected electron density was found in the active site and was assigned as a bicarbonate ion based on its planar shape and hydrogen-bonding pattern. The authors suggest that the bicarbonate ion might act as a general base to abstract a proton from the methylated-carbocation intermediate to allow cyclopropane ring formation (65). Alternatively, it might serve to stabilize the transition state via an electrostatic interaction.

The Use of Onium Chalcogen Effects in other Enzyme Systems. Whether onium chalcogen effects will prove to be a generally useful tool for elucidating the mechanisms of AdoMet-dependent reactions remains to be determined. As described for thio effects in phosphoryl transfer reactions, a meaningful interpretation of any effect will probably require caution as well as additional information from supporting methods. However, in contrast to sulfur substitution for oxygen in phosphoryl transfer reactions, onium chalcogen substitution would appear to be less invasive, since the chalcogen itself would not be expected to interact directly with active site amino acids in the ground state or transition state of the reaction. The most significant change would be simply in the size of the molecule.

The employment of onium chalcogens of AdoMet would appear to be most useful in enzyme systems such as CFA synthase, wherein the mode of reactivity is unclear and formation of a sulfonium ylide is a mechanistic possibility. Two similar systems deserve mention. The first is the enzyme QueA, which catalyzes the penultimate step in the biosynthesis of queuosine, a hypermodified nucleoside found in the anticodons of certain tRNAs (67). This nucleoside contains a cyclopentenediol group attached to a (7-amino-methyl)-7-deazaguanine core structure termed preQ1. QueA transfers the ribosyl moiety of AdoMet to preQ1 with release of adenine and methionine and concomitant formation of an exopoxy carbocycle. Recent mechanistic investigations of this enzyme are most consistent with formation of a sulfonium ylide as a key step in catalysis (68).

The second system involves the biosynthesis of the polycyclopropane fatty acid derivatives FR-900848 and U-106305 from *Streptovorticillium fervens* and *Streptomyces*. The former is a potent antibiotic against filamentous fungi, while the latter is an inhibitor of cholesteryl ester transfer protein (69, 70). It has been proposed that a polyenoic fatty acid side chain of U-106305 is the substrate for cyclopropane formation via cationic intermediates, since the fatty acid is derived from acetate units as in polyketide and fatty acid biosynthesis (69). A contrasting proposal suggests that cyclopropane formation in U-106305 derives from sulfonium ylide formation, followed by attack of the carbanion on the α/β unsaturated thioester while the fatty acid is appended to the acyl carrier protein (71). The large number of uncharacterized AdoMet-dependent reactions and the intrinsic diversity of the reactivity of the sulfonium substituent portend new and exciting chemistry to be unraveled soon.

ACKNOWLEDGMENT

We thank Dr. Henry Gong of the Penn State University Geology department for assistance with metal analysis.

SUPPORTING INFORMATION AVAILABLE

Typical HPLC traces for the CFA synthase assay in the absence (Figure S2) and presence (Figure S1) of AdoHcys nucleosidase, as well as a typical GC trace of the CFA synthase assay (Figure S3). This information is available free of charge via the Internet at <http://pubs.acs.org>.

REFERENCES

- Grogan, D. W., and Cronan, J. E., Jr. (1997) Cyclopropane ring formation in membrane lipids of bacteria, *Microbiol. Mol. Biol. Rev.* 61, 429–441.
- Law, J. H. (1971) Biosynthesis of cyclopropane rings, *Acc. Chem. Res.* 4, 199–203.
- Cronan, J. E., Jr., Nunn, W. D., and Batchelor, J. G. (1974) Studies on the biosynthesis of cyclopropane fatty acids in *Escherichia coli*, *Biochim. Biophys. Acta* 348, 63–75.
- Wang, A. Y., and Cronan, J. E., Jr. (1994) The growth phase-dependent synthesis of cyclopropane fatty acids in *Escherichia coli* is the result of an *RpoS*(*KatF*)-dependent promoter plus enzyme instability, *Mol. Microbiol.* 11, 1009–1017.
- Taylor, F., and Cronan, J. E., Jr. (1976) Selection and properties of *Escherichia coli* mutants defective in the synthesis of cyclopropane fatty acids, *J. Bacteriol.* 125, 518–523.
- Grogan, D. W., and Cronan, J. E., Jr. (1986) Characterization of *Escherichia coli* mutants completely defective in synthesis of cyclopropane fatty acids, *J. Bacteriol.* 166, 872–877.
- Chang, Y. Y., and Cronan, J. E., Jr. (1999) Membrane cyclopropane fatty acid content is a major factor in acid resistance of *Escherichia coli*, *Mol. Microbiol.* 33, 249–259.
- Brennan, P. J., and Nikaido, H. (1995) The envelope of mycobacteria, *Annu. Rev. Biochem.* 64, 29–63.
- Chatterjee, D. (1997) The mycobacterial cell wall: structure, biosynthesis and sites of drug action, *Curr. Opin. Chem. Biol.* 1, 579–588.
- Glickman, M. S., Cox, J. S., and Jacobs, W. R. (2000) A novel mycolic acid cyclopropane synthetase is required for cording, persistence, and virulence of *Mycobacterium tuberculosis*, *Mol. Cell* 5, 717–727.
- George, K. M., Yuan, Y., Sherman, D. R., and Barry, C. E. (1995) The biosynthesis of cyclopropanated mycolic acids in *Mycobacterium tuberculosis* – identification and functional analysis of *Cma2*, *J. Biol. Chem.* 270, 27292–27298.
- Yuan, Y., Lee, R. E., Besra, G. S., Belisle, J. T., and Barry, C. E. (1995) Identification of a gene involved in the biosynthesis of cyclopropanated mycolic acids in *Mycobacterium tuberculosis*, *Proc. Natl. Acad. Sci. U.S.A.* 92, 6630–6634.
- Glickman, M. S., Cahill, S. M., and Jacobs, W. R. (2001) The *Mycobacterium tuberculosis* *cmaA2* gene encodes a mycolic acid trans-cyclopropane synthetase, *J. Biol. Chem.* 276, 2228–2233.
- Taylor, F. R., and Cronan, J. E., Jr. (1979) Cyclopropane fatty acid synthase of *Escherichia coli*. Stabilization, purification, and interaction with phospholipid vesicles, *Biochemistry* 18, 3292–3300.
- Yuan, Y., Mead, D., Schroeder, B. G., Zhu, Y., and Barry, C. E., 3rd. (1998) The biosynthesis of mycolic acids in *Mycobacterium tuberculosis*. Enzymatic methyl(ene) transfer to acyl carrier protein bound meromycolic acid in vitro, *J. Biol. Chem.* 273, 21282–21290.
- Polacheck, J. W., Tropp, B. E., and Law, J. H. (1966) Biosynthesis of cyclopropane compounds. VIII. The conversion of oleate to dihydrosterulate, *J. Biol. Chem.* 241, 3362–3364.
- Buist, P. H., and MacLean, D. B. (1982) Biosynthesis of cyclopropane fatty acids. II. Mechanistic studies using methionine labeled with 1, 2, and 3 deuterium atoms in the methyl group, *Can. J. Chem.* 60 (4), 371–378.
- Ohkita, M., Nishida, S., and Tsuji, T. (1995) in *The Chemistry of the Cyclopropyl Group* (Rappoport, Z., Ed.) pp 261–318, John Wiley & Sons Ltd, New York.

19. Wessjohann, L. A., Brandt, W., and Thiemann, T. (2003) Biosynthesis and metabolism of cyclopropane rings in natural compounds, *Chem. Rev.* 103, 1625–1648.
20. Pohl, S., Law, J. H., and Ryhage, R. (1963) The path of hydrogen in the formation of cyclopropane fatty acids, *Biochim. Biophys. Acta* 70, 583–585.
21. Cheng, J.-P., Liu, B., Zhao, Y., Sun, Y., Zhang, X.-M., and Lu, Y. (1999) Effects of adjacent onium cations and remote substituents on the H–A⁺ bond equilibrium acidities in dimethyl sulfoxide solution. An extensive ylide thermodynamic stability scale and implication for the importance of resonance effect on ylide stabilities, *J. Org. Chem.* 64, 604–610.
22. Cohen, T., Herman, G., Chapman, T., and Kuhn, D. (1974) A laboratory model for the biosynthesis of cyclopropane rings. Copper-catalyzed cyclopropanation of olefins by sulfur ylides, *J. Am. Chem. Soc.* 96, 5627–5628.
23. Nes, W. D. (2003) Enzyme mechanisms for sterol C-methylations, *Phytochemistry* 64, 75–95.
24. Akhtar, M., and Jones, C. (1978) Some biological transformations involving unsaturated linkages: the importance of charge separation and charge neutralization in enzyme catalysis, *Tetrahedron* 34, 813–832.
25. Yuan, Y., and Barry, C. E., 3rd. (1996) A common mechanism for the biosynthesis of methoxy and cyclopropyl mycolic acids in *Mycobacterium tuberculosis*, *Proc. Natl. Acad. Sci. U.S.A.* 93, 12828–12833.
26. Iwig, D. F., and Booker, S. J. (2004) Insight into the polar reactivity of the onium chalcogen analogues of S-adenosyl-L-methionine, *Biochemistry* 43, 13496–13509.
27. Sambrook, J., Fritsch, E. F., and Maniatis, T. (1989) *Molecular Cloning: A Laboratory Manual*, 2nd ed., Vol. 1, Cold Spring Harbor Laboratory Press, Plainview, NY.
28. Heinrikson, R. L., and Meredith, S. C. (1984) Amino acid analysis by reverse-phase high-performance liquid chromatography: pre-column derivatization with phenylisothiocyanate, *Anal. Biochem.* 136, 65–74.
29. Gill, S. C., and von Hippel, P. H. (1989) Calculation of protein extinction coefficients from amino acid sequence data, *Anal. Biochem.* 182, 319–326.
30. Stewart, J. C. (1980) Colorimetric determination of phospholipids with ammonium ferrothiocyanate, *Anal. Biochem.* 104, 10–14.
31. Lotta, T., Vidgren, J., Tilgmann, C., Ulmanen, I., Melen, K., Julkunen, I., and Taskinen, J. (1995) Kinetics of human soluble and membrane-bound catechol O-methyltransferase: a revised mechanism and description of the thermolabile variant of the enzyme, *Biochemistry* 34, 4202–4210.
32. Wang, A. Y., Grogan, D. W., and Cronan, J. E., Jr. (1992) Cyclopropane fatty acid synthase of *Escherichia coli*: deduced amino acid sequence, purification, and studies of the enzyme active site, *Biochemistry* 31, 11020–11028.
33. Markham, G. D. (September 2002) S-Adenosylmethionine, *Nature Encyclopedia of Life Sciences*, Nature Publishing Group, London, <http://www.els.net/doi:10.1038/npg.els.0000662>.
34. Segel, I. H. (1975) *Enzyme Kinetics: Behavior and Analysis of Rapid Equilibrium and Steady-State Enzyme Systems*, John Wiley & Sons, Ltd., New York.
35. Voet, D., and Voet, J. G. (2004) *Biochemistry*, 3rd ed., Vol. 1, John Wiley & Sons, Ltd., New York.
36. Berg, O. G., and Jain, M. K. (2002) *Interfacial Enzyme Kinetics*, John Wiley & Sons, Ltd., New York.
37. Parks, L. W., and Schlenk, F. (1958) Formation of alpha-amino-gamma-butyrolactone from S-adenosylmethionine, *Arch. Biochem. Biophys.* 75, 291–292.
38. Parks, L. W., and Schlenk, F. (1958) The stability and hydrolysis of S-adenosylmethionine: isolation of S-ribosylmethionine, *J. Biol. Chem.* 230, 295–305.
39. Wu, S.-E., Huskey, W. P., Borchardt, R. T., and Schowen, R. L. (1983) Chiral instability at sulfur of S-adenosylmethionine, *Biochemistry* 22, 2828–2832.
40. Hoffman, J. L. (1986) Chromatographic analysis of the chiral and covalent instability of S-adenosyl-L-methionine, *Biochemistry* 25, 4444–4449.
41. Takusagawa, F., Fujioka, M., Spies, A., and Schowen, R. L. (1998) *Comprehensive Biological Catalysis: A Mechanistic Reference*, Vol. 1, Academic Press, San Diego, CA.
42. Takata, Y., Konishi, K., Gomi, T., and Fujioka, M. (1994) Rat guanidinoacetate methyltransferase. Effect of site-directed alteration of an aspartic acid residue that is conserved across most mammalian S-adenosylmethionine-dependent methyltransferases, *J. Biol. Chem.* 269, 5537–5542.
43. Lindstrom, W. M., Jr., Flynn, J., and Reich, N. O. (2000) Reconciling structure and function in *HhaI* DNA cytosine-C-5 methyltransferase, *J. Biol. Chem.* 275, 4912–4919.
44. Malygin, E. G., Zinoviev, V. V., Evdokimov, A. A., Lindstrom, W. M., Jr., Reich, N. O., and Hattman, S. (2003) DNA (cytosine-N⁴-) and -(adenine-N⁶-) methyltransferases have different kinetic mechanisms but the same reaction route. A comparison of *M.BamHI* and T4 Dam, *J. Biol. Chem.* 278, 15713–15719.
45. Reich, N. O., and Mashhoon, N. (1993) Presteady-state kinetics of an S-adenosylmethionine-dependent enzyme. Evidence for a unique binding orientation requirement for *EcoRI* DNA methyltransferase, *J. Biol. Chem.* 268, 9191–9193.
46. Chen, L., MacMillan, A. M., Chang, W., Ezaz-Nikpay, K., Lane, W. S., and Verdine, G. L. (1991) Direct identification of the active-site nucleophile in a DNA (cytosine-5)-methyltransferase, *Biochemistry* 30, 11018–11025.
47. Wu, J. C., and Santi, D. V. (1987) Kinetic and catalytic mechanism of *HhaI* methyltransferase, *J. Biol. Chem.* 262, 4778–4786.
48. Polesky, A. H., Dahlberg, M. E., Benkovic, S. J., Grindley, N. D., and Joyce, C. M. (1992) Side chains involved in catalysis of the polymerase reaction of DNA polymerase I from *Escherichia coli*, *J. Biol. Chem.* 267, 8417–8428.
49. Herschlag, D., Piccirilli, J. A., and Cech, T. R. (1991) Ribozyme-catalyzed and nonenzymatic reactions of phosphate diesters: rate effects upon substitution of sulfur for a nonbridging phosphoryl oxygen atom, *Biochemistry* 30, 4844–4854.
50. Zhao, L., Liu, Y., Bruzik, K. S., and Tsai, M. D. (2003) A novel calcium-dependent bacterial phosphatidylinositol-specific phospholipase C displaying unprecedented magnitudes of thio effect, inverse thio effect, and stereoselectivity, *J. Am. Chem. Soc.* 125, 22–23.
51. Borchardt, R. T. (1979) Mechanism of alkaline hydrolysis of S-adenosyl-L-methionine and related sulfonium nucleosides, *J. Am. Chem. Soc.* 101, 458–463.
52. Marcus, R. A. (1968) Theoretical relations among rate constants, barriers, and Brønsted slopes of chemical reactions, *J. Phys. Chem.* 72, 891–899.
53. Gerlt, J. A., Kozarich, J. W., Kenyon, G. L., and Gassman, P. G. (1991) Electrophilic catalysis can explain the unexpected acidity of carbon acids in enzyme-catalyzed reactions, *J. Am. Chem. Soc.* 113, 9667–9669.
54. Gerlt, J. A., and Gassman, P. G. (1993) Understanding the rates of certain enzyme-catalyzed reactions: proton abstraction from carbon acids, acyl-transfer reactions, and displacement reactions of phosphodiester, *Biochemistry* 32, 11943–11952.
55. Crosby, J., and Stirling, C. J. M. (1970) Elimination and addition reactions. Part XIX. Elimination of phenoxide from β -substituted ethyl phenyl ethers: the nature of activation in 1,2-elimination, *J. Chem. Soc. B*, 671–679.
56. Hegazi, M. F., Borchardt, R. T., and Schowen, R. L. (1979) α -Deuterium and carbon-13 isotope effects for the methyl transfer catalyzed by catechol-O-methyl transferase EC-2.1.1.6 s_{N2} -like transition state, *J. Am. Chem. Soc.* 101 (15), 4359–4365.
57. Vogel, P. (1985) *Carbocation Chemistry*, Vol. 21, Elsevier Science Publishing Company, Inc., New York.
58. Proudfoot, J. R., Li, X., and Djerassi, C. (1985) Minor and trace sterols from marine invertebrates. 50. Stereostructure and synthesis of nicaesterol, a novel cyclopropane-containing sponge sterol, *J. Org. Chem.* 50, 2026–2030.
59. Proudfoot, J. R., and Djerassi, C. (1987) Synthesis and stereochemistry of 23,24-dihydrocalysterol: implications for marine sterols of a unified biosynthetic scheme involving protonated cyclopropanes, *J. Chem. Soc., Perkin Trans. 1*, 1283–1290.
60. Giner, J. L., and Djerassi, C. (1991) Biosynthetic studies of marine lipids. 31. Evidence for a protonated cyclopropyl intermediate in the biosynthesis of 24-propylidenecholesterol, *J. Am. Chem. Soc.* 113, 1386–1393.
61. Lee, J. K., and Houk, K. N. (1997) Cation cyclization selectivity: variable structures of protonated cyclopropanes and selectivity control by catalytic antibodies, *Angew. Chem., Int. Ed. Engl.* 36, 1003–1005.
62. Li, T., Janda, K. D., and Lerner, R. A. (1996) Cationic cyclopropanation by antibody catalysis, *Nature* 379, 326–327.
63. March, J. (1985) *Advanced Organic Chemistry: Reactions, Mechanisms, and Structure*, John Wiley and Sons Ltd., New York.

64. Chong, S.-L., and Franklin, J. L. (1972) Heats of formation of protonated cyclopropane, methylcyclopropane, and ethane, *J. Am. Chem. Soc.* **94**, 6347–6351.
65. Huang, C. C., Smith, C. V., Glickman, M. S., Jacobs, W. R., and Sacchettini, J. C. (2002) Crystal structures of mycolic acid cyclopropane synthases from *Mycobacterium tuberculosis*, *J. Biol. Chem.* **277**, 11559–11569.
66. Dougherty, D. A. (1996) Cation- π interactions in chemistry and biology: a new view of benzene, Phe, Tyr, and Trp, *Science* **271**, 163–168.
67. Slany, R. K., Bosl, M., and Kersten, H. (1994) Transfer and isomerization of the ribose moiety of AdoMet during the biosynthesis of queuosine tRNAs. A new unique reaction catalyzed by the QueA protein from *Escherichia coli*, *Biochimie* **76**, 389–393.
68. Kinzie, S. D., Thern, B., and Iwata-Reuyl, D. (2000) Mechanistic studies of the tRNA-modifying enzyme QueA: a chemical imperative for the use of AdoMet as a “ribosyl” donor, *Org. Lett.* **2**, 1307–1310.
69. Kuo, M. S., Zielinski, R. J., Cialdella, J. I., Marschke, C. K., Dupuis, M. J., Li, G. P., Kloosterman, D. A., Spilman, C. H., and Marshall, V. P. (1995) Discovery, isolation, structure elucidation, and biosynthesis of U-106305, a cholesteryl ester transfer protein inhibitor from UC 11136, *J. Am. Chem. Soc.* **117**, 10629–10634.
70. Yoshida, M., Ezaki, M., Hashimoto, M., Yamashita, M., Shigematsu, N., Okuhara, M., Kohsaka, M., and Horikoshi, K. (1990) A novel antifungal antibiotic, FR-900848. I. Production, isolation, physico-chemical and biological properties, *J. Antibiot. (Tokyo)* **43**, 748–754.
71. Barrett, A. G. M., Hamprecht, D., White, A. J. P., and Williams, D. J. (1997) Iterative cyclopropanation: a concise strategy for the total synthesis of the hexacyclopropane cholesteryl ester transfer protein inhibitor U-106305, *J. Am. Chem. Soc.* **119**, 8608–8615.

BI048692H